UNIVERSIDADE DE SÃO PAULO

INSTITUTO DE FÍSICA
CAIXA POSTAL 66318
05389-970 SÃO PAULO - SP
BRASIL

PUBLICAÇÕES

IFUSP/P-1164

EFFECT OF DELAY ON THE BOUNDARY OF THE BASIN OF ATTRACTION IN A SELF-EXCITED SINGLE NEURON

K. Pakdaman and **J.-F. Vibert**
Falcuté de Médecine Saint-Antoine 27, rue Chaligny
75571 Paris Cedex 12, France

C.P. Malta
Instituto de Física, Universidade de São Paulo

C. Grotta-Ragazzo
Instituto de Matemática e Estatística
Universidade de São Paulo
CP 66281, 05389-970, São Paulo, BRASIL

Junho/1995

Effect of Delay on the Boundary of the Basin of Attraction in a Self-Excited Single Neuron

K. Pakdaman†, C.P. Malta‡, C. Grotta-Ragazzo* and J.-F. Vibert†

† B3E, INSERM U 263, ISARS
Faculté de Médecine Saint-Antoine
27, rue Chaligny
75571 Paris Cedex 12 FRANCE

‡ Instituto de Física
Universidade de São Paulo
CP 66318, 05389-970 São Paulo, BRASIL

* Instituto de Matemática e Estatística
Universidade de São Paulo
CP 66281, 05389-970 São Paulo, BRASIL

Correspondence should be addressed to:
K. Pakdaman
B3E, INSERM U263
Faculté de Médecine Saint-Antoine
27, rue Chaligny
75571 Paris Cedex 12, FRANCE
tel: 33-1-44738430
fax: 33-1-44738462
email: pakdaman@b3e.jussieu.fr

Abstract: Little attention has been paid in the past to the effects of inter-unit transmission delays on the boundary of the basin of attraction of stable equilibrium points in neural networks. As a first step towards a better understanding of the influence of delay, we study the dynamics of a single neuron with a delayed excitatory self-connection. In this system, most trajectories converge to stable equilibrium points for any delay value. However, changing the delay modifies the boundary of the basin of attraction of these stable equilibrium points. Our results suggest that when dealing with networks with delay, it is not only important to study the effect of the delay on the asymptotic behavior of the system, but also on the boundary of the basin of attraction of the equilibria.

1 Introduction

The time it takes for a signal to be transmitted from one neuron to another, referred to here as delay, can influence the behavior of biological neural network models (an der Heiden, 1981; Plant, 1981; Gerstner & van Hemmen, 1992; Vibert *et al.*, 1994; Pakdaman *et al.*, 1995). It has been shown that the adjunction of delay to discrete time networks made of binary units enables them to store time-varying sequences (Sompolinsky and Kanter, 1986; Herz *et al.*, 1988). In analog neural networks composed of units with nonlinear graded responses, the same phenomenon may deteriorate the network performance. For example, in an associative memory network, in which stable equilibrium points are used for storing information (Hirsch, 1989), increasing the delay beyond a critical value may render a locally stable equilibrium point unstable. Such considerations as well as other applications have motivated a number of studies on the asymptotic behavior of neural networks with delay (Marcus and Westerwelt, 1989; Marcus *et al.*, 1991; Roska *et al.*, 1992; Bélair, 1993; Burton, 1993; Civalleri *et al.*, 1993; Gilli, 1993; Roska *et al.*, 1993; Gopalsamy and He, 1994; Ye *et al.*, 1994). By studying the local stability of the equilibria, criteria have been derived to avoid delay induced instabilities in some networks (Marcus and Westerwelt, 1989; Bélair, 1993). It has even been possible to provide constraints on network parameters so that all or almost all trajectories converge to stable equilibrium points in networks with delay (Roska *et al.*, 1992; Bélair, 1993; Burton, 1993; Civalleri *et al.*, 1993; Roska *et al.*, 1993; Gopalsamy and He, 1994; Ye *et al.*, 1994). However, even in such (quasi) convergent networks, important features in the system's dynamics may still depend on the delay value. For instance, changing the delay can alter [illegible]dary of the basins of attraction of the stable equilibrium points. This can be of prime importance in an associative memory network: the position of the basin boundaries determines in which basin a given information falls. Thus changing the shape of the basin boundaries alters the classification.

In this paper we provide an example to illustrate how the delay may alter the basin boundary. To this end, we study the dynamics of a single neuron with a delayed excitatory self-connection. This system has been chosen because *i)* it is simple enough so that thorough theoretical and numerical analysis of its dynamics are possible, and *ii)* most trajectories converge to stable equilibrium points for any value of the delay, allowing to focus on the effect of delay on the basin boundary.

In section 2 we present the neuron model. The stationary regime is described in section 3. The boundary of the basin of attraction of a locally asymptotically stable equilibrium point is estimated for different delay values in section 4. Details of the mathematical aspects are left to appendices.

2 The neuron model

In the nonlinear graded response model (NGRM), a neuron is described by its activation at time t, noted $a(t)$, and a sigmoidal output function $\sigma(a)$. A decay rate γ is also implemented in the model. For more details and references on the NGRM see (Hopfield & Tank, 1986; Pasemann, 1993). We consider a neuron that has a delayed self-connection with strictly positive connection weight W and delay A. The neuron receives a constant input K. The neuron activation evolves according to the following delay differential equation (DDE):

$$\frac{da}{dt}(t) = -\gamma a(t) + K + W\sigma(a(t-A)) \tag{1}$$

Where σ is defined by:

$$\sigma(a) = \frac{1}{1+e^{-a}} \tag{2}$$

Here, the initial condition of the system is constituted by the history of the neuron activation during a time interval corresponding to the delay. Thus, initial conditions for DDE (1) are the continuous functions ϕ defined on the interval $[-A, 0]$ of length equal to the delay (appendix A). Since changing the delay alters this interval, we need to specify how to identify initial conditions for a given delay with those for another value. In this paper we use two methods. An initial condition defined for a given delay (Fig. 1-1 middle) is restricted to a shorter interval (Fig. 1-2 top) and defines thus an initial condition for a shorter delay (appendix B.1). The second method is theoretically advantageous. In this method, a change of variable rescales the time unit to the delay (Fig. 1-3 bottom), so that for all delays, initial conditions are defined on the same interval of unit length $[-1, 0]$ (appendix B.2).

FIGURE 1 HERE

One of the important properties of DDE (1) is that it preserves the order of initial conditions. That is, if an initial condition is larger than another one then the corresponding solutions will have the same property. The activation corresponding to the larger initial condition remains larger than the one corresponding to the smaller initial condition (appendix A.3).

3 The stationary regime

The asymptotic behavior of DDE (1) is analyzed in appendix A. The results can be summarized as follows. For $W < 4\gamma$ there is one globally asymptotically stable point, noted x_0. For $W > 4\gamma$, there are two input values K_- and K_+ such that when either $K < K_-$ or $K > K_+$, there is one globally asymptotically stable point, also noted

x_0; and for $K_- < K < K_+$, the system is bistable: there are two locally asymptotically stable equilibria, noted x_1 and x_3, and one unstable equilibrium point noted x_2, with $x_1 < x_2 < x_3$. For the bistable system most trajectories converge to the stable equilibrium points in the sense that the union of the basins of attraction of the two stable equilibrium points is a dense open set. In fact the orbit of a constant initial condition converges to x_1, x_2 or x_3 depending on whether it is smaller than, equal to or larger than x_2 respectively. The situation is similar for an arbitrary initial condition ϕ. There is a unique real number $b(\phi)$, such that the orbit of $\phi + c$ tends to x_1 (resp. x_3) if and only if $c < b(\phi)$ (resp. $c > b(\phi)$). For $c = b(\phi)$, the solution going through $\phi + c$ oscillates indefinitely around x_2. (appendix A.3). For instance, for a constant initial condition ϕ taking the value q, we have $b(\phi) = x_2 - q$.

FIGURE 2 HERE

Figure 2 shows the temporal evolution of the activation $a(t)$ for several initial conditions for a bistable system. It can be seen that the orbits of initial conditions that are either smaller or larger than the unstable point x_2 converge to the stable equilibrium point x_1 or x_3 respectively. Moreover these solutions can be bounded by the solutions of properly chosen constant initial conditions. The situation is more complex for an initial condition ϕ that oscillates around x_2, that is when there is at least one value θ such that $\phi(\theta) = x_2$, with $-A < \theta < 0$. In this case the solution going through ϕ may oscillate transiently and then converge to one of the two stable equilibrium points (x_1 or x_3) or it may even oscillate indefinitely around x_2. Such an oscillatory solution is not stable. It belongs to the boundary separating the basins of attraction of the two stable equilibrium points.

FIGURE 3 HERE

In figure 3, examples of the temporal evolution of solutions for initial conditions oscillating around x_2 are shown. The figure is based on numerical investigations carried out for two delay values ($A = 1$ and $A = 5$). For this system we have $W > 4\gamma$ and $K_- < K < K_+$, so that there are two locally stable ($x_1 \simeq -2.6$ and $x_3 \simeq 2.6$) and one unstable ($x_2 = 0$) equilibrium points. The initial condition is set to $\phi(t) = \sin(10t)$ for $-A \leq t \leq 0$ with $A = 1$ (dotted line), and $A = 5$ (thin line). The initial condition for the shorter delay is a restriction of the initial condition for the longer delay as exemplified in figures 1-1 and 1-2. It can be seen that for the short delay (dotted line) the solution converges rapidly to the lower locally stable equilibrium point x_1, whereas for the longer delay (thin line) the system displays transient oscillations before converging (far from the end of the figure) to the upper locally stable equilibrium point x_3. The thick line represents the solution going through the initial condition $\psi(t) = \sin(2t)$ for $-5 \leq t \leq 0$. This initial condition corresponds to the function $\phi(t) = \sin(10t)$ $(-1 \leq t \leq 0)$ when the unit time is rescaled to the delay as described at the end of section 2. The initial condition for the dotted line is a rescaling of the initial condition for the thick line as exemplified in figures 1-1 and 1-3. In this case there are

also transient oscillations before the system converges to the lower locally stable equilibrium point x_1.

4 The boundary of the basin of attraction

Based on the description of the asymptotic behavior of solutions given in section 3, it can be seen that the basin of attraction of x_1 and x_3 are the sets of initial conditions ϕ such that $b(\phi) > 0$ and $b(\phi) < 0$ respectively. The basin boundary is the set of the zeros of b. This set is formed by the solutions that oscillate indefinitely around x_2.

As can be seen in figure 3, the equilibrium point to which the orbit of an initial condition that oscillates around x_2 converges, may switch from either of the two stable equilibrium points to the other as the delay is changed. This example gives evidence for the basin boundary being delay dependent. In this section we investigate how the basin boundary is modified when the delay is changed.

As the space of the initial conditions of DDE (1) is an infinite dimensional space (appendix A), it is not possible to visualize the basin boundary in that space. To overcome this difficulty, a family of initial conditions depending on one parameter is selected $(\phi_\alpha(t))$. For each value of the real parameter α we note $\beta(\alpha) = b(\phi_\alpha)$. The orbit of an initial condition $\phi(t) = \phi_\alpha(t) + c$ converges to x_1 or x_3 depending on whether c is strictly smaller than or strictly larger than $\beta(\alpha)$. Thus the graph of $\beta(\alpha)$ in the (α, c) parameter plane represents the boundary of the basin of attraction for initial conditions ϕ defined as above: points with coordinates (α, c) situated "below" (resp. "above") the graph of $\beta(\alpha)$ correspond exactly to the functions ϕ with parameter α and bias c ($\phi(t) = \phi_\alpha(t) + c$) whose orbit tends to x_1 (resp. x_3). This allows to compute the basin boundary for a special family of initial conditions, as a function of the parameter α and to represent it as a one dimensional graph. This method can be easily generalized to families depending on two parameters $(\phi_{\alpha,\omega}(t))$ for which the basin boundary $\beta(\alpha, \omega) = b(\phi_{\alpha,\omega})$ is a two dimensional surface in the (α, ω, c) parameter space.

FIGURE 4 HERE

Figure 4 shows estimations of the basin boundary for affine functions $\phi_\alpha(t) = \alpha t$, for $-1 \leq t \leq 0$. For a given delay A, we solve the rescaled equation (Equ. (18) in appendix B.2) with the initial condition $\phi_\alpha + c$. We note $\beta_r(\alpha)$ the value of β obtained for this family of initial conditions. It has been estimated for two different delays $A = 0.5$ (dashed lines), $A = 15$ (solid lines). The thick lines were obtained by solving numerically the DDE and the thin lines result from the theoretical approximation (Equ. (17) in appendix A.3). This approximation of $\beta_r(\alpha)$ is a linear function. It fits the numerical result over some interval of α around 0. However the length of this interval shrinks as the delay is decreased. For $\alpha = 0$, the initial condition is constant and all four graphs of β go through $\beta_r(0) = x_2$ as expected. DDE (1) preserves the order of initial conditions, so that $\beta_r(\alpha)$ is an increasing function of α, and its graph has a positive slope. For very short delays close to zero, the slope tends to zero and the graph of $\beta_r(\alpha)$ is close to the straight horizontal line going through $x_2 = 0$. This slope increases with the delay.

The basin boundary can also be estimated for a restricted (if $A < 1$) or extended (if $A > 1$) initial condition defined by: $\phi_\alpha(t) = \alpha t$ for $-A \leq t \leq 0$. We note $\beta_e(\alpha)$ the value obtained in this way. Then we have:

$$\beta_e(A\alpha) = \beta_r(\alpha) \tag{3}$$

This relation allows to obtain an estimation of the basin boundary for the first method of comparison – restriction – from the results presented in the previous paragraph. It should be noted that such a relation does not exist for an arbitrary family of initial conditions.

FIGURE 5 HERE

Figure 5 shows estimations of the basin boundary for sine initial conditions ($\phi_{\alpha,\omega}(t) = \alpha \sin(\omega t)$, $-1 \leq t \leq 0$). For each value of (α, ω), the value $\beta_r(\alpha, \omega)$ is shown for delays $A = 0.5$ (Fig. 5-A) and $A = 5$ (Fig. 5-B). Both theoretical approximations and the results of the numerical resolution of the DDE are represented for each delay. In both figures, the theoretical estimation matches the numerical one for low amplitude sine functions (α close to zero). For a fixed ω, $\beta_r(\alpha, \omega)$ is a monotonous function of α, that either increases or decreases from zero as α increases from zero. For a fixed α, the boundary displays oscillations that are damped as ω increases (Fig. 5-C). The main difference due to the change in the delay is in the amplitude of the "waves" of the boundary surface. For sake of brevity only basin boundaries for rescaled initial conditions were presented. For restricted or extended initial conditions the results are similar. In fact there is a relation similar to equation (3) linking the basins boundary of rescaled sine initial conditions to that of extended or restricted sine initial conditions.

5 Discussion

In this paper, we studied the dynamics of a single neuron with a delayed excitatory self-connection. The system we have considered is simple and allows us to carry out a precise theoretical and numerical characterization of the boundary of the basin of attraction of a locally stable equilibrium point. The analysis methods relied mainly on specific properties of DDE (1) (*i.e.* it generates an order preserving semiflow (appendix A.3)) and may not be adequate for the study of networks commonly used in applications that may have both positive and negative connection weights. It is known that scalar systems with a delayed feedback can display complex dynamics depending on both the feedback nature – positive, negative or mixed (an der Heiden & Mackey, 1982; Malta & Grotta-Ragazzo, 1991) and the number of feedback loops (Glass & Malta, 1990; Grotta-Ragazzo & Malta, 1992).

Moreover the basin boundary in such systems can have an intricate structure (Losson *et al.*, 1993). Therefore a network made of a large number of units with both delayed excitatory and inhibitory connections may display complex behaviors (Marcus *et al.*, 1991; Gilli, 1993). Nevertheless, our results suggest that even in a quasi convergent system with delay, the boundary of the basin of attraction of the stable equilibria may depend on the value of the delay.

The change of the basin boundary with the delay was established for non-constant initial conditions. In our example, the asymptotic behavior of constant initial conditions is not affected by the delay and the boundary of the basin of attraction would not depend on the delay if the initial conditions were restricted to constant functions. However this is a special property of the system we considered and a larger network with delay having both positive and negative connection weights may not display the same behavior.

Studying the orbits of non-constant initial conditions poses the problem of comparing initial conditions for various delay values. In our work we proposed two methods that were adequate for our purpose. However there is no unique way to compare initial conditions, and other methods may be developed that would be better suited for particular applications.

The influence of delay on network dynamics has also been investigated in networks composed of a slightly different version of the NGRM, usually referred to as the "shunting model" (Destexhe & Gaspard, 1993; Destexhe, 1994; Houweling, 1994; Lourenço & Babloyantz, 1994). The results presented in this paper can be easily adapted to the dynamics of a single shunting model neuron with a delayed excitatory self-connection receiving a constant input (appendix C).

6 Conclusion

For neural networks designed to converge to equilibria, such as associative memories, the rate of error in retrieving the relevant information depends on the shape of the basin of attraction of the equilibrium points. In this paper we have shown that even in a quasi convergent system, the boundary of the basins may be modified by the presence of delays. This can deteriorate the performance if the delay is not under control. However our work was based on the behavior of a single neuron and represents only the first step towards the study of the influence of delay on the basin boundaries in neural networks.

Acknowledgment: The authors would like to thank Dr. E. Av-Ron and Pr. O. Arino for helpful comments. This work was partially supported by USP/COFECUB under project U/C 9/94. One of us (CPM) is also partially supported by CNPq (the Brazilian Research Council).

7 Reference

Arino, O. (1993). A note on "the discrete Lyapunov function ...". *Journal of Differential Equations.* **104,** 169–181.

Arino, O. & Benkhalti, R. (1988). Periodic solutions for $\dot{x}(t) = \lambda f(x(t), x(t-1))$. *Proceedings of the Royal Society of Edinburgh, section A.* **109,** 245–260.

Arino, O. & Séguier, P. (1979). Existence of oscillating solutions for certain differential equations with delay. H.O. Peitgen & H.-O. Walther (Eds) *Functional Differential Equations and Approximation of Fixed Points,* Lecture Notes in Mathematics vol. **730** (pp. 46–64). Berlin: Springer–Verlag.

Bélair, J. (1993). Stability in a model of a delayed neural network. *Journal of Dynamics and Differential Equations.* **5,** 607–623.

Brauer, F. (1979). Characteristic return times for harvested population models. *Mathematical Biosciencces.* **45,** 295–311.

Brauer, F. (1979). Decay rates for solutions of a class of differential-difference equations. *SIAM Journal of Mathematical Analysis.* **10,** 783–788.

Burton, T.A. (1993). Averaged neural networks. *Neural Networks.* **6,** 677–680.

Civalleri, P.P., Gilli, M. & Pandolfi, L. (1993). On stability of cellular neural networks with delay. *IEEE Transactions on Circuits and Systems_I: Fundamental Theory and Applications.* **40,** 157–165.

Cowan, J. & Ermentrout G.B. (1978). Some aspects of the 'eigenbehavior' of neural nets. In S.A. Levin (Ed.) *Studies in Mathematical Biology, part I,* 67–117, The Mathematical Association of America.

Destexhe, A. (1994). Oscillations, complex spatiotemporal behavior, and information transport in networks of excitatory and inhibitory neurons. *Physical Review E.* **50,** 1594–1606.

Destexhe, A. & Gaspard, P. (1993). Bursting oscillations from a homoclinic tangency in a time delay system. *Physics Letters A.* **173,** 386-391.

Gerstner, W. & van Hemmen, J.L. (1992). Associative memory in a network of 'spiking' neurons. *Network.* **3,** 139–164.

Gilli, M. (1993). Strange attractors in delayed cellular neural networks. *IEEE Transactions on Circuits and Systems_I: Fundamental Theory and Applications.* **40,** 849–853.

Glass, L. & Malta, C.P. (1990). Chaos in multi-looped negative feedback systems. *Journal of Theoretical Biology.* **145,** 217–223.

Gopalsamy, K. & He, X.-Z. (1994). Stability in asymmetric Hopfield nets with transmission delays. *Physica D.* **76,** 344–358.

Grotta-Ragazzo, C. & Malta, C.P. (1992). Singularity structure of the Hopf bifurcation surface of a differential equation with two delays. *Journal of Dynamics and Differential Equations.* **4,** 617–650.

Hale, J.K. & Verduyn Lunel, S.M. (1993). Introduction to Functional Differential Equations. Applied Mathematical Sciences vol. **99.** New-York: Springer-Verlag.

an der Heiden, U. (1981). *Analysis of neural networks.* Lecture Notes in Biomathematics vol. **35.** Berlin ; New York : Springer-Verlag.

an der Heiden, U. & Mackey, M.C. (1982). The dynamics of production and destruction: analytic insight into complex behavior. *Journal of Mathematical Biology.* **16,** 75–101.

Herz, A., Sulzer, B., Kühn, R. & Van Hemmen, J.L. (1988). The Hebb rule: storing static and dynamic objects in an associative neural network. *Europhysics Letters.* **7,** 663–669.

Hirsch, M.W. (1989). Convergent activation dynamics in continuous time networks. *Neural Networks.* **2,** 331–350.

Hopfield, J.J. & Tank, D.W. (1986). Computing with neural circuits: a model. *Science* **233,** 625–633.

Houweling. A.R. (1994). The effects of interneural time delay in a simple two neuron shunting model. Personal communication.

Losson, J., Mackey, M.C. & Longtin, A. (1993). Solution multistability in first-order nonlinear differential delay equations. *Chaos.* **3,** 167–176.

Lourenço, C. & Babloyantz, A. (1994). Control of chaos in networks with delay: a model for synchronization of cortical tissue. *Neural Computation.* **6**, 1141–1154.

Malta, C.P. & Grotta-Ragazzo, C. (1991). Bifurcation structure of scalar delayed equations. *International Journal of Bifurcation and Chaos.* **1**, 657–665.

Malta, C.P. & Teles, M.L.S. Delayed differential equations: comparison of different numerical integration methods. *in preparation.*

Marcus, C.M., Waugh, F.R. & Westervelt, R.M. (1991). Nonlinear dynamics and stability of analog neural networks. *Physica D.* **51**, 234–247.

Marcus, C.M. & Westervelt, R.M. (1989). Stability of analog neural networks with delay. *Physical Review A.* **39**, 347–359.

Pakdaman, K.; Vibert, J.-F.; Boussard, E. & Azmy, N. (1995). Single neuron with recurrent excitation: effect of the transmission delay. *Neural Networks.* in press.

Pasemann, F. (1993). Dynamics of a single neuron model. *International Journal of Bifurcation and Chaos.* **3**, 271–278.

Plant, R.E. (1981). A FitzHugh differential-difference equation modeling recurrent neural feedback. *SIAM Journal of Applied Mathematics.* **40**, 150–162.

Roska, T., Wu, C.F., Balsi, M. & Chua, L.O. (1992). Stability and dynamics of delay-type general and cellular neural networks. *IEEE Transactions on Circuits and Systems_I: Fundamental Theory and Applications.* **39**, 487–490.

Roska, T., Wu, C.F. & Chua, L.O. (1993). Stability of cellular neural networks with dominant nonlinear and delay-type templates. *IEEE Transactions on Circuits and Systems_I: Fundamental Theory and Applications.* **40**, 270–272.

Smith, H. (1987). Monotone semiflows generated by functional differential equations. *Journal of Differential Equations.* **66**, 420–442.

Sompolinsky, H. & Kanter, I. (1986). Temporal association in asymmetric neural network. *Physical Review Letter.* **57**, 2861–2864.

Vibert, J.-F., Pakdaman, K. & Azmy, N. (1994). Inter-neural delay modification synchronizes biologically plausible neurons. *Neural Networks.* **7**, 589–607.

Ye, H., Michel, A.N. & Wang, K. (1994). Global stability and local stability of Hopfield neural networks with delays. *Physical Review E.* **50**, 4206–4213.

A Asymptotic Stability

The neuron activation evolves according to the following DDE:

$$\frac{da}{dt}(t) = -\gamma a(t) + K + W\sigma(a(t-A)) \tag{4}$$

Where σ is the sigmoidal function defined by:

$$\sigma(a) = \frac{1}{1+e^{-a}} \tag{5}$$

and W and A are strictly positive real numbers. This system is similar to the positive feedback loop with a piecewise constant transfer function studied by an der Heiden and Mackey (1982).

Let $C[-A,0]$ be the space of continuous real functions of the interval $[-A,0]$. For ϕ in $C[-A,0]$, there exists a unique real function $a(t,\phi)$ on the interval $[-A,+\infty)$, such that $a(t,\phi)=\phi(t)$ for $-A \le t \le 0$, and $a(t,\phi)$ satisfies equation (4) for $t \ge 0$ (Hale and Verduyn Lunel, 1993). For such a solution of the DDE, we note $a_t(\phi)$ the element of $C[-A,0]$, defined by $a_t(\phi)(\theta) = a(t+\theta,\phi)$, for $-A \le \theta \le 0$.

A.1 Local stability

In this section, the local stability of the solutions taking a constant value, i.e. equilibrium points, of DDE (4) is studied. A function taking the value x, that is $a(t) = x$ for all $t \ge -A$, is a solution of equation (4) if and only if x is a zero of Z, the right hand side of equation (4):

$$Z(x) = -\gamma x + K + W\sigma(x) \tag{6}$$

The number and value of the zeros of Z depend on the values of the parameters (γ, W, K). See also (Cowan & Ermentrout, 1978; Pasemann, 1993). The parameter set can be separated into two regions, one in which the equation has a unique zero, noted x_0, and another such that it has three zeros $x_1 < x_2 < x_3$.

More precisely we have:

- For $0 \leq W < 4\gamma$, Z has a unique zero noted x_0.
- For $W > 4\gamma$, let:

$$
\begin{aligned}
K_-(\gamma, W) &= -\gamma Log(\frac{W-2\gamma+\sqrt{W(W-4\gamma)}}{2\gamma}) - \frac{W-\sqrt{W(W-4\gamma)}}{2} \\
K_+(\gamma, W) &= \gamma Log(\frac{W-2\gamma+\sqrt{W(W-4\gamma)}}{2\gamma}) - \frac{W+\sqrt{W(W-4\gamma)}}{2}
\end{aligned} \tag{7}
$$

  1. For either $K < K_-$ or $K > K_+$, Z has a unique zero also noted x_0.
  2. For $K_- < K < K_+$, Z has three zeros noted $x_1 < x_2 < x_3$.

For the study of the local exponential asymptotic stability of each equilibrium point, the real parts of the solutions λ of the characteristic equation (8) at the equilibrium point are examined.

$$\lambda + \gamma - W\sigma'(x_i)e^{-\lambda A} = 0 \tag{8}$$

A.1.1 The locally stable points

For the equilibria x_0, x_1 and x_3 the following inequality holds:

$$\gamma > W\sigma'(x_i) > 0 \quad \text{for } i \text{ in } \{0, 1, 3\} \tag{9}$$

From inequality (9) it can be deduced that the characteristic equation (8) admits a real strictly negative solution, noted $\mu_A(x_i)$ and that all its other solutions are complex with real parts smaller than $\mu_A(x_i)$. This ensures that these constant solutions be locally exponentially asymptotically stable (Hale and Verduyn Lunel, 1993).

Moreover for $\Delta \geq A$ we have:

$$-\gamma \leq \mu_A(x_i) \leq \mu_\Delta(x_i) < 0 \tag{10}$$

and in fact $\mu_\Delta(x_i)$ increases and tends to zero as Δ increases and tends to infinity.

In summary, the local asymptotic stability of the stable equilibrium points of the system does not depend on the delay.

A.1.2 The unstable point

At x_2 the situation is different, we have:

$$\gamma < W\sigma'(x_2) \tag{11}$$

From this inequality it can be deduced that the characteristic equation admits a real strictly positive solution, noted $\nu_A(x_2)$ and all its other solutions are complex with real parts smaller than $\nu_A(x_2)$. Therefore the equilibrium point x_2 is a locally unstable point (Hale and Verduyn Lunel, 1993). Using the same notations and definitions as for μ we have:

$$0 < \nu_\Delta(x_2) \leq \nu_A(x_2) \tag{12}$$

and in fact $\nu_A(x_2)$ decreases and tends to zero as Δ increases and tends to infinity.

The characteristic equation at x_2 may have other solutions with positive real parts depending on the delay value. In fact there is an increasing sequence of delays A_k, defined by:

$$
\begin{aligned}
&\tan(A_k\sqrt{W^2\sigma'(x_2)^2 - \gamma^2}) = \sqrt{W^2\sigma'(x_2)^2 - \gamma^2}/\gamma \\
&\text{with } 2k\pi\sqrt{W^2\sigma'(x_2)^2 - \gamma^2} < A_k < (2k + 1/2)\pi\sqrt{W^2\sigma'(x_2)^2 - \gamma^2}
\end{aligned} \tag{13}
$$

such that there is a pair of complex conjugate solutions of the characteristic equation crossing the imaginary axis from left to right at A_k.

The number of solutions with positive real parts determines the dimension of the unstable space of the unstable equilibrium point of the linearized equation, and it also gives some indication about the extent of instability of the nonlinear equation near this point (Hale and Verduyn Lunel, 1993). Therefore increasing the delay renders the unstable point more unstable.

A.2 Return and escape times

The solutions of the characteristic equation at the equilibria change with the delay, even though for the stable equilibrium points their real parts remain negative for all delay values. This is important for evaluating the response of the system to perturbations. A system, stabilized at a locally stable equilibrium point x_i (i in $\{0, 1, 3\}$), returns to it when perturbed with a characteristic return time $T_r(x_i, A)$ (Brauer, 1979a-b) and we have:

$$T_r(x_i, A) = -A/\mu_A(x_i) \tag{14}$$

$T_r(x_i, A)$ is an increasing function of A tending to infinity.

In the same way we can define a characteristic escape time $T_e(x_2, A)$ for the unstable point x_2:

$$T_e(x_2, A) = A/\nu_A(x_2) \tag{15}$$

$T_e(x_2, A)$ is an increasing function of A tending to infinity.

Therefore the characteristic return and escape times close to the equilibria are lengthened and tend to infinity as the delay is increased.

A.3 Global stability

Let ϕ_0 and ϕ_1 be two elements in $\mathcal{C}[-A,0]$, then we say that ϕ_0 is larger (resp. strictly larger) than ϕ_1 noted $\phi_0 \geq \phi_1$ (resp. $\phi_0 >> \phi_1$) if for all θ in $[-A,0]$ we have $\phi_0(\theta) \geq \phi_1(\theta)$ (resp. $\phi_0(\theta) > \phi_1(\theta)$). DDE (4) generates an order preserving semiflow: for ϕ_0 and ϕ_1 in $\mathcal{C}[-A,0]$:

$$\text{if } \phi_0 \geq \phi_1 \text{ and } \phi_0 \neq \phi_1, \text{ then for } t > 2A \quad a_t(\phi_0) >> a_t(\phi_1) \tag{16}$$

Therefore the orbit of an arbitrary initial condition ϕ in $\mathcal{C}[-A,0]$ is bounded by the orbits of two constant initial conditions.

The fact that DDE (4) generates an order preserving semiflow strongly limits the possible asymptotic behaviors of the solutions (Smith, 1987; Roška *et al.*, 1992).

- For $W < 4\gamma$, all solutions converge uniformly asymptotically to x_0.
- For $W > 4\gamma$

  1. For either $K < K_-$ or $K > K_+$, all solutions converge uniformly asymptotically to x_0.
  2. For $K_- < K < K_+$, the union of the basins of attraction of x_1 and x_3 is a dense open subset of $\mathcal{C}[-A,0]$. F[illegible] in $\mathcal{C}[-A,0]$, there is a unique real number $b(\phi)$ such that $a_t(\phi+c)$ tends asymptotically to x_1 (resp. x_3) for all $c < b(\phi)$ (resp. $c > b(\phi)$); where for a real number c, we note $\phi + c$ the element of $\mathcal{C}[-A,0]$ defined by $(\phi+c)(t) = \phi(t) + c$, for $-A \leq t \leq 0$. $a(t,(\phi + b(\phi))$ oscillates around x_2, in the sense that the function $a(t,(\phi+b(\phi)) - x_2$ has at least one zero on each interval $kA < t < (k+1)A$, for $k \geq -1$. The boundary of the basin of attraction of the two locally stable equilibrium points is formed by such oscillating solutions. Properties of these oscillations, such as convergence to x_2 and periodicity, depend on the instability of x_2, and have been studied in (Arino and Séguier, 1979; Arino and Benkhalti, 1988; Arino, 1993).

     The function b from $\mathcal{C}[-A,0]$ to the real line is continuous. The boundary of the basins of attraction of the two locally stable equilibria is the closed set $\{\phi, \text{ such that } b(\phi) = 0\}$.

     We approximate $b(\phi)$ by the projection of ϕ onto the most unstable eigendirection of the linearized equation at x_2 along the eigenspace of all the other solutions of the characteristic equation (8) (see (Hale & Verduyn Lunel, 1993)).

$$b(\phi) = \phi(0) - x_2 + W\sigma'(x_2)e^{-\nu.A}\int_{-A}^{0}(\phi(u) - x_2)e^{-\nu.u}du \tag{17}$$

where ν stands for ν_A, the real solution of the characteristic equation, which is also the solution with the largest real part (appendix A.1). This approximation is satisfactory near the unstable equilibrium. When the characteristic equation has a single solution with a positive real part, then the basin boundary coincides with the stable manifold of the unstable equilibrium point x_2. In this case, the zeros of the above approximation of b represent the tangent space to the stable manifold at x_2.

B Comparing initial conditions

The space of initial conditions of DDE (4) is $\mathcal{C}[-A,0]$ the infinite dimensional space of continuous functions on the interval $[-A,0]$. This space depends on the delay A. In order to compare the orbits for various delays, we have to be able to compare functions in $\mathcal{C}[-A,0]$ for different values of A.

In this paper the comparison is based on the two following methods.

B.1 Restricting the initial condition

Let ϕ be a function on the interval $[-A,0]$, then the restriction ψ of ϕ to the interval $[-A',0]$, where $A' < A$ belongs to $\mathcal{C}[-A',0]$. In order to see how the delay changes the basin boundaries, we can compare the orbit of the initial condition ϕ (for a system with a delay A) with that of the initial condition ψ (for a system with a delay A'). Note that a restricted function ψ corresponds to infinitely many functions ϕ.

B.2 Rescaling of the initial conditions

In DDE (4), we make a change of variable by setting $t' = t/A$, and we rename the parameters: $\tau = \gamma A$, $K' = K/\gamma$, and $W' = W/\gamma$. The transformed equation is thus:

$$\frac{1}{\tau}\frac{d\hat{a}}{dt'}(t') = -\hat{a}(t') + K' + W'\sigma(\hat{a}(t'-1)) \tag{18}$$

An initial condition ϕ of DDE (4) is transformed to an initial condition ψ for DDE (18) by setting $\psi(s) = \phi(As)$, for $-1 \leq s \leq 0$; so that ψ belongs to $\mathcal{C}[-1,0]$, which is independent from A. Therefore one way to evaluate the effect of the delay on the behavior of the system, is to study the dynamics of DDE (18) for various values of the parameter τ.

C The shunting model

In the shunting model, the neuron activation evolves according to the following DDE:

$$\frac{da}{dt}(t) = -\gamma a(t) + K + W(E - a(t))\sigma(a(t - A)) \quad (19)$$

where $E > 0$ is the positive reversal potential. Let $K' = K/\gamma$, we further suppose $E > K'$.

For any function ϕ in $C[-A, 0]$, there is a unique solution of DDE (19) $a(t, \phi)$ going through ϕ, and there is a time $T \geq -A$ such that the activation is below the reversal potential after T, that is for all $t \geq T$, $a(t, \phi) < E$. The restriction of the set of initial conditions of DDE (19) to continuous functions on the interval $[-A, 0]$ that are smaller than E, generates a strictly order preserving semiflow.

Based on the above considerations, and the study of the local stability of the equilibria of DDE (19), we can state the following. Let K_0 be the unique solution of the following equation, such that $K_0 < E$.

$$(e^{x+2} - 1)(E - x) + 4 = 0 \quad (20)$$

For $K' > K_0$ there is one globally asymptotically stable point, noted x_0, with $K' < x_0 < E$. For $K' > K_0$, there are two positive weight values W_- and W_+ such that when either $W < W_-$ or $W > W_+$, there is one globally asymptotically stable point, also noted x_0 with $K' < x_0 < E$; and for $W_- < W < W_+$, the system is bistable: there are two locally asymptotically stable equilibria, noted x_1 and x_3, and one unstable equilibrium point noted x_2, with $K' < x_1 < x_2 < x_3 < E$. For the bistable system most trajectories converge to the stable equilibrium points in the sense that the union of the basins of attraction of the two stable equilibrium points is a dense open set. The basin boundary can be characterized in the same way as for the NGRM.

D Numerical solution

The numerical solution of DDE (1) is obtained by discretization of time which makes the problem finite. The equation is then integrated by using the GEAR corrector formula which can be easily adapted to integrating DDEs when nonlinearities are restricted to the terms which contain the delay (Malta & Teles, in preparation).

The time step used was 10^{-4}. The calculations were carried with double precision on DEC AXP and Microvax 3300.

FIGURE LEGENDS

and

FIGURES

Figure 1: *Comparing initial conditions*

How to obtain an initial condition for a DDE with delay equal to 1*, from an initial condition defined for a delay* $A > 1$*. A continuous function defined on the interval* $[-A, 0]$ **(1)** *(middle), is either restricted to a shorter interval* **(2)** *(top) — here to* $[-1, 0]$ *— or rescaled to* $[-1, 0]$ **(3)** *(bottom) to define an initial condition for a DDE with delay equal to* 1*. Abscissae: time* t*, ordinates: activation.*

Figure 2: *Examples of solutions*

The time evolution of solutions for 5 initial conditions are represented. In this case the system has two locally asymptotically stable equilibrium points at $x_1 \simeq -2.6$ *and* $x_3 \simeq 2.6$*, and an unstable equilibrium point at* $x_2 = 0$*. Trajectories of initial conditions lower (resp. larger) than* x_2 *converge to* x_1 *(resp.* x_3*). The trajectory of an initial condition that oscillates around* x_2 *may converge to either of the stable equilibrium points or oscillate indefinitely. The trajectory of an initial condition bounded by two constant initial conditions remains bounded between their trajectories. Abscissae: time* t*; ordinates: activation* $a(t)$*. Parameters used for the simulation* $\gamma = 1$*,* $W = 6$*,* $K = -3$ *with delay* $A = 1$*. The initial conditions are:* $\alpha \sin(\omega t) + \beta$ *for* $(\alpha = 0, \beta = -1.6)$*,* $(\alpha = 0, \beta = -0.8)$*,* $(\alpha = 0.4, \beta = -1.2)$*,* $(\alpha = 0.4, \beta = 0)$*,* $(\alpha = 0.4, \beta = 1.2)$*.*

Figure 3: *Examples of solutions for oscillating initial conditions*

This system has an unstable point at $x_2 = 0$*, and two locally stable points at* $x_1 \simeq -2.6$ *and* $x_3 \simeq 2.6$*. The initial condition is set to* $\phi(t) = \sin(10t)$ *for* $-A \leq t \leq 0$ *with* $A = 1$ *(dotted line), and* $A = 5$ *(thin line). The thick line represents the solution going through the initial condition* $\psi(t) = \sin(2t)$ *for* $-5 \leq t \leq 0$*. This initial condition corresponds to the function* $\phi(t) = \sin(10t)$ $(-1 \leq t \leq 0)$ *when the unit time is rescaled to the delay. Same coordinates and same parameters* γ*,* W *and* K *as in figure 2.*

Figure 4: *Basin boundaries for affine functions*

The boundary $\beta_r(\alpha)$ *of the basin of attraction for affine initial conditions with slope* α *and bias c,* $\phi_\alpha(t) = \alpha t + c$ $(-1 \leq t \leq 0)$*, is shown for* $A = 0.5$ *(dashed line) and* $A = 15.0$ *(solid line). The thick lines correspond to the numerical result and the thin lines correspond to the theoretical approximation (Equ. (17)). Abscissae: slope* α*, ordinates: bias c. Same parameters* γ*,* W *and* K *as in figure 2.*

Figure 5:

The boundary $\beta_r(\alpha, \omega)$ *of the basin of attraction for sine initial conditions with amplitude* α*, angular velocity* ω *and bias c:* $\phi_{\alpha,\omega}(t) = \alpha \sin(\omega t)$ $(-1 \leq t \leq 0)$*, is shown for* $A = 0.5$ *(A) and* $A = 5$ *(B). C: cross sections at* $\alpha = 5$ *of* $\beta(\alpha, \omega)$*. The thick lines correspond to the numerical result and the thin lines correspond to the theoretical approximation (Equ. (17)). Solid lines for the long delay* $(A = 5)$ *and dashed lines for the short delay* $(A = 0.5)$*. Abscissae: angular velocity* ω*, ordinates: bias c. Same parameters* γ*,* W *and* K *as in figure 2.*

Figure 1

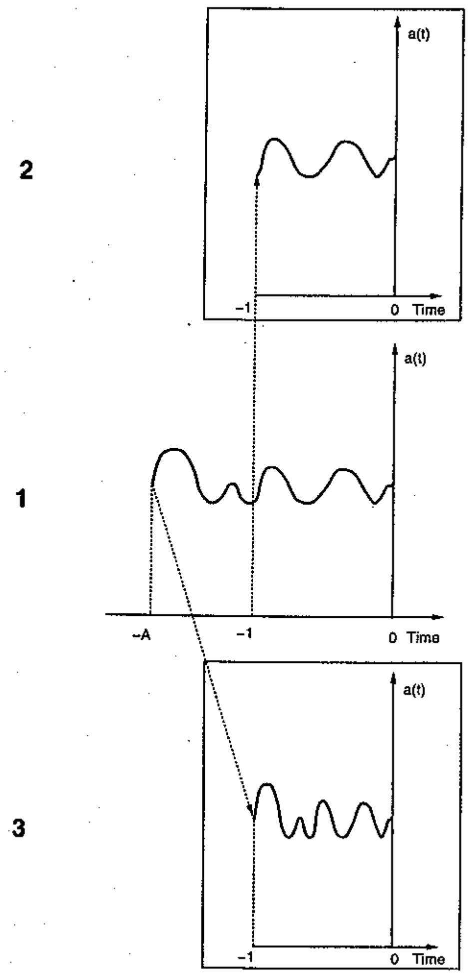

Figure 2

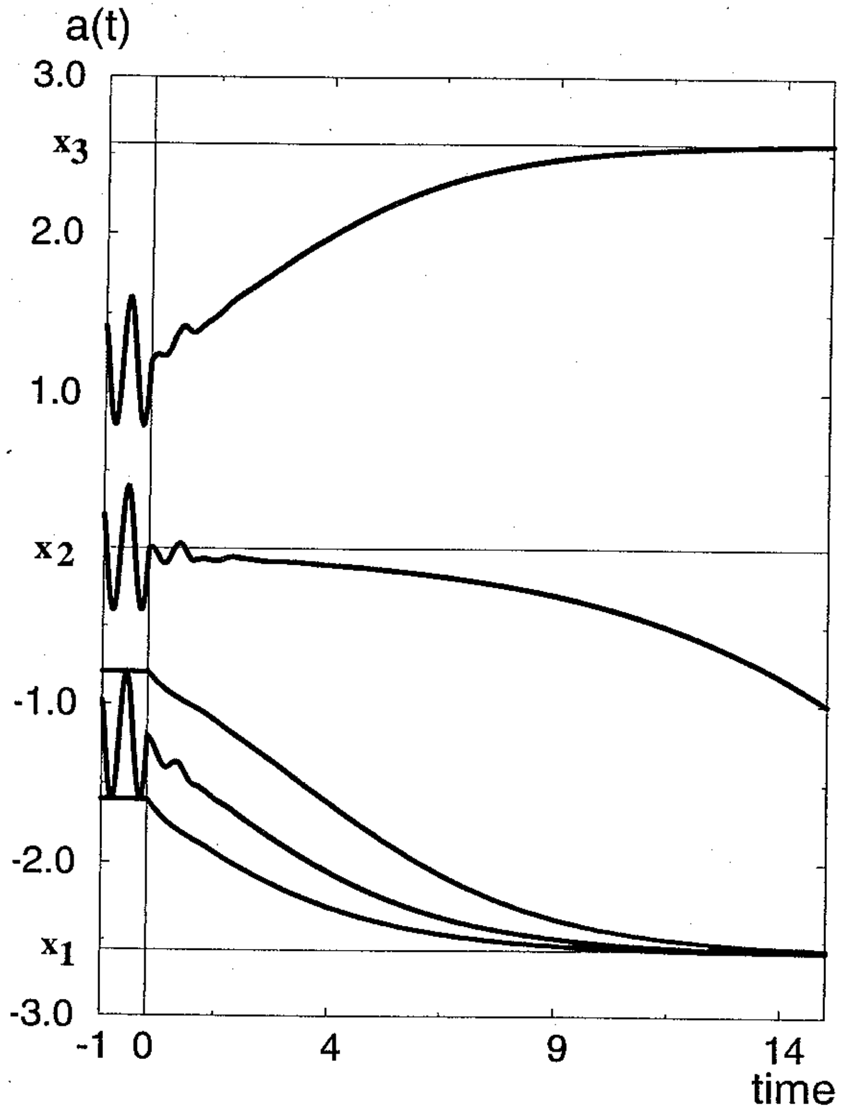

Figure 3

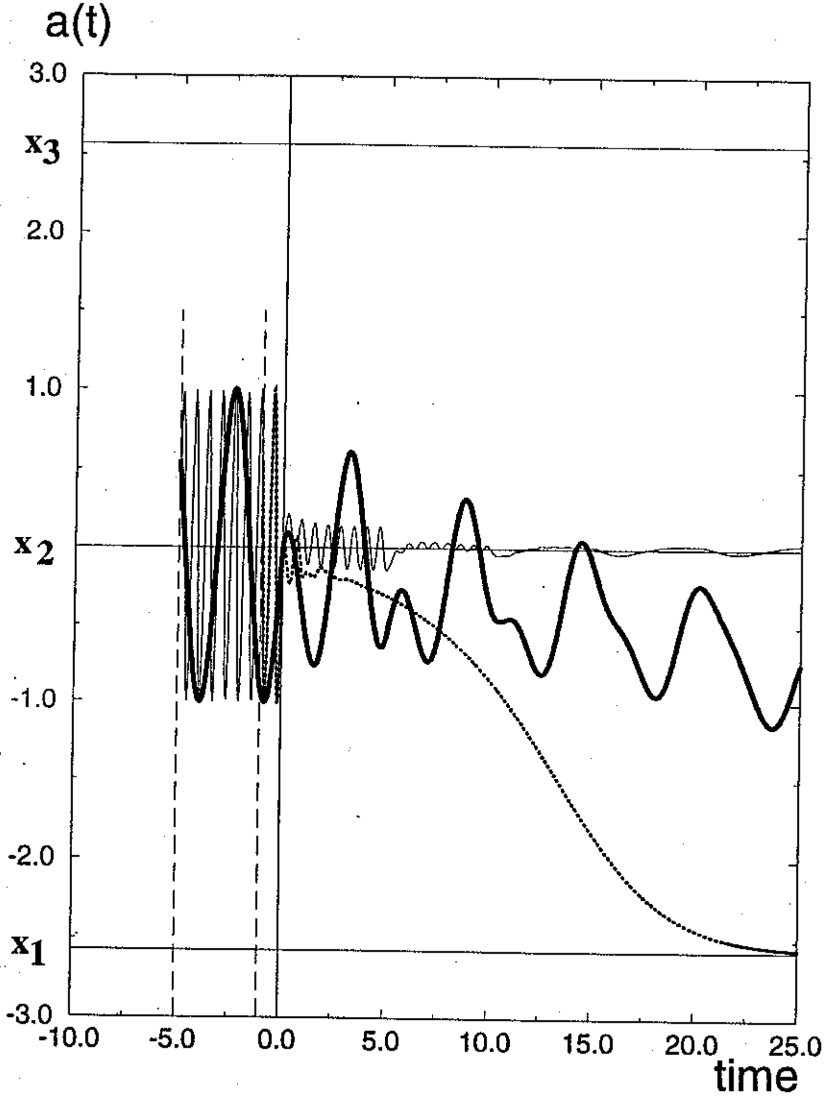

Figure 4

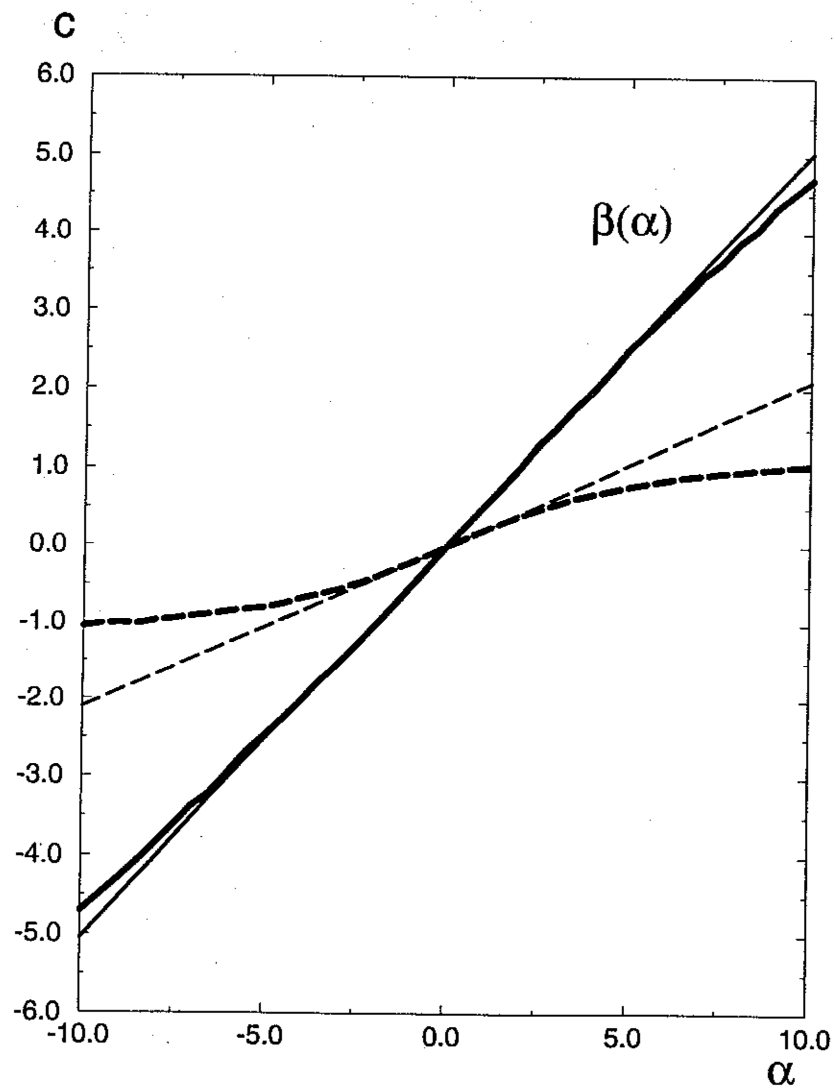

Figure 5